

Measuring Optical Component Radiation Damage

1 August 2017

Derek Wenzl, Richard J Tesarek
Cuyahoga Community College-Cleveland
Fermilab National Accelerator Laboratory

Abstract

Scintillator based detectors are used to monitor beam losses in the Fermilab accelerator complex. These detectors are approximately 500 times faster than traditional ionization chamber loss monitors and can see beam losses 20 nanoseconds apart. These fast loss monitors are used in areas of the accelerator known to be sources of heavy beam loss and as such, are exposed to high doses of radiation. Over time, radiation exposure reduces the ability of optical components to transmit light by darkening the material. The most dramatic effects are seen in the optical cement and light guide materials comprising the detector. We explore this darkening effect by measuring the transmittance spectra of the detector materials for varying irradiation exposures. Presented here, are the optical transmittance spectra for a variety of radiation exposures and optical materials. The data has revealed an epoxy which withstands exposure far better than traditional optical cements.



Figure 1: Diagram of a detector module with component breakdown.

Introduction

Scintillator based detectors or fast loss monitors (FLM) used at Fermilab are essential to improving the performance of the accelerator. Capable of measuring signals that are 20 nanoseconds apart, detector modules provide high temporal resolution data. These detectors are placed in locations in the Booster which are known to be areas of heavy beam loss, such as near the collimators. This exposure to radiation darkens the materials that light propagates through, reducing the transmittance. We are looking for materials that are more radiation tolerant.

A detector module is comprised of two scintillation counters. The components of a counter are: plastic scintillator material (EJ-200) [1], acrylic light guide and cookie, optical cement (EJ-500) [1], and a photomultiplier tube (PMT). These components are fastened to each other using optical cement.

As ionizing radiation escapes the booster and makes contact with the scintillator material, a track of ionized atoms are brought to a higher energy state. Recombination of electrons and ions causes the scintillator material used in our detectors to emit photons in the shorter end of the visible light spectrum. Light is channeled through the scintillator, into the light guide and cookie, and finally into the PMT.

Optical cement offers structural support and serves to be the optical coupling of the detector. The optical cements have been chosen such that their index of refraction falls between that of the scintillator and light guide material. The indices of refraction for EJ-200 and acrylic are 1.58 and 1.488 respectively. Joining materials with similar indices of refraction maximizes transmittance between the interfaces. We calculated this using Fresnel's equation:

$$R = \left(\frac{n_2 \cos \theta_2 - n_1 \cos \theta_1}{n_2 \cos \theta_2 + n_1 \cos \theta_1} \right)^2,$$

where R is the reflection coefficient, n_2 and n_1 are indices of refraction for the materials, θ_1 is the incident angle, and θ_2 is the angle of transmittance. Transmittance is $1 - \text{Reflectance}$.

Scintillators, light guides, and optical cement darken over time and from exposure to radiation [2]. This darkening impedes light transmission to the photomultiplier tubes. The darkest part of the assembly is the adhesive which joins the material. To quantify this darkening effect, we want to measure the transmittance of a material as a function of wavelength after irradiation.

Table 1: Detector Material Samples

Sample	Abbr.	Ind. of Refraction
Acrylic [3]	(A)	1.4880
BC-600 [4]	(BC)	1.5710
EJ-500 [1]	(EJ)	1.5742
Mirror Coat [1]	(MC)	1.5607
Polycarbonate	(PC)	1.5860
General Purpose Epoxy [5]	(GP)	1.5666
UV-Resistive Acrylic [3]	(UVRA)	1.4862

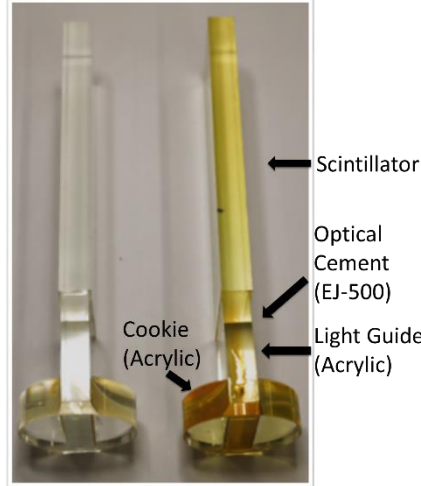


Figure 2: Scintillator and light guides, low and high exposure.

Method

We prepared samples of optical cement and light guide material, listed in Table 1. Six cylindrical, identically prepared samples were made of each material, with dimensions of 7.62 mm thick and a diameter of 19.05 mm. Before exposure, we measured the transmittance for each of the samples. Transmittance measurements were made using an Agilent 8453 UV-visible Spectroscopy System [6]. Each sample was provided with a label and an alignment mark.

For transmittance measurements, the sample was placed in the spectrophotometer with the alignment mark facing up, and the label to the right of the mark. Once a spectrum was recorded, the sample was rotated 90° clockwise and another spectrum was taken. This process was repeated until the sample returned to its initial position. Taking measurements over the different orientations was done to understand the effects of non-uniformity of the samples.

After measuring the transmittances, one sample of each material was placed into one of seven wells of six identical Delrin sample holders. The base of a sample holder is 8.89 cm x 8.89 cm x 1.905 cm thick, and the lid has the same length and width but is .9525 cm thick. Lastly, underneath the middle sample in each of the holders, a .02 cm x 1 cm x 1 cm silicon photodiode was placed in order to measure the radiation dose.

On 10/8/16, sample holders 1, 4 and 3, 5 were mounted to detectors downstream of collimators 6B and 6A, respectively. These locations were chosen as they are known to be areas of high beam loss in the booster. The remaining two sample holders (6 and 7) were used as control samples.

Once sample holders are harvested, we measure the dose from the photodiodes. To obtain the dose, we reverse bias the photodiodes by 80 volts and measure leakage current. [7]. This is possible due to the linear relationship between leakage current and dose, as shown in Figure 3. The dose is measured as a particle fluence which is calculated as follows:

$$\Phi = \frac{\Delta I}{V\alpha},$$

where Φ is Fluence (MIPs/ cm²), ΔI is the change of current (A), V is volume (cm³), and α is the damage coefficient (3.0x10⁻¹⁷ A/cm).

On 3/1/2017, we harvested sample holder number 4 and measured the transmittance and dosimetry. At this time, we also measured the transmittance of the unirradiated samples again. The method used to do this was the same as mentioned above in the pre-irradiation measurements. Dosimetry of this harvest date was 3.6 x 10¹⁴ ionizing particles/cm².

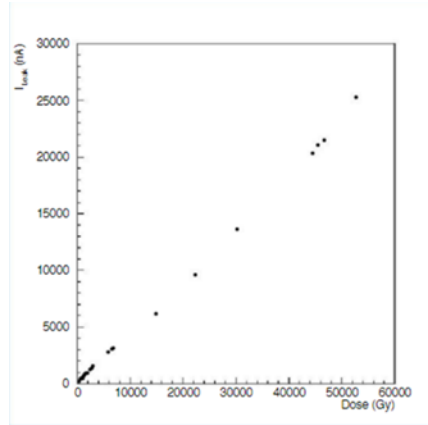


Figure 3: Leakage current as a function of radiation dose from data collected inside the CDF detector.
Courtesy of CDF Radiation Monitoring Group.

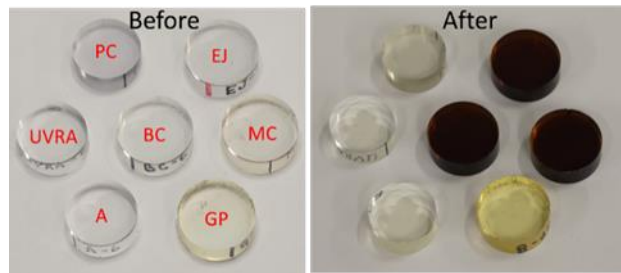


Figure 4: Samples before and after exposure to radiation in the Booster. Sample orientation same in both photos.

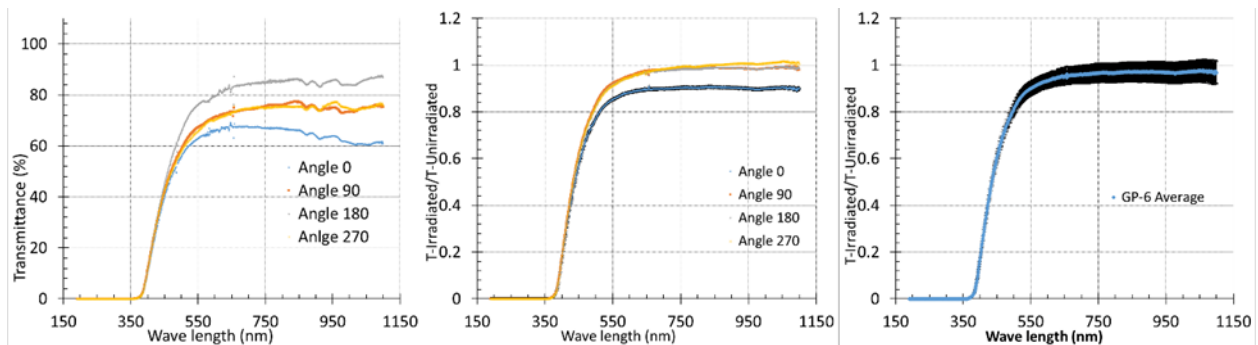


Figure 5: Transmittance spectra after radiation exposure (Left). Irradiated/pre-irradiated transmittance spectra (Center). Transmittance ratio spectrum averaged over angles (Right). All plots are GP

On 4/26/2017, sample holder number 1 was removed and underwent the same procedure listed above, with a measured dosimetry of 3.4×10^{14} ionizing particles/cm². Sample holder mounting position, radiation field shape, and a temperature dependence when measuring dosimetry are possible reasons for the difference in dose rate experienced between sample holders 1 and 4, but these effects need to be further explored.

On 7/12/2017, the last two sample holders (3 and 5) were harvested and underwent the same process for measuring transmittance and dosimetry. The dosimetry for sample holders 3 and 5 was 6.4×10^{14} and 8.3×10^{14} respectively.

Analysis

Analysis of the transmittance spectrum data proceeds as follows. To evaluate the darkening effect, we plotted the transmittance as a function of wavelength. Figure 5 shows a representative transmittance spectrum for the GP sample. The irradiated/pre-irradiated transmittance ratio is formed to better quantify the change in transmittance. The error bars shown on angle zero are nearly the size of the data points. An average over all angles is performed to provide a single spectrum. Similar plots to those shown in Figure 5 were made for each material tested.

Comparing the plots and data for GP and EJ samples reveals that after exposure, GP still transmits light below 400 nm while EJ darkened such that the transmittance threshold is over 550 nm. Bialkali photocathodes are most sensitive around 420 nm. Table 2 shows the transmittance of each of the samples at 420 nm. The approximate thickness of all the samples tested was 7.62 mm. The approximate thickness of epoxy applied to the coupling points on a detector is 0.1 mm. The transmittance values listed in Table 2 were found using the formula:

$$T(t) = e^{-t/\tau},$$

where τ is $t/\ln(T)$ (mm), T is Transmittance, and t is thickness of sample (mm).

Table 2: Transmittance at 420 nm. Thickness of samples were 7.62 mm. Typical thickness of optical cement used in detector is .1 mm.

Sample	T(.1mm)	T(7.62mm)	T(10mm)
A	0.99286 ± 0.00031	0.579254 ± 0.013860	0.488433 ± 0.015337
BC	0.91974 ± 0.00068	0.001704 ± 0.000097	0.000233 ± 0.000017
EJ	0.90092 ± 0.00365	0.000352 ± 0.000109	0.000029 ± 0.000012
MC	0.91342 ± 0.00051	0.001007 ± 0.000043	0.000117 ± 0.000007
PC	0.98954 ± 0.00042	0.448804 ± 0.014417	0.349448 ± 0.014731
GP	0.98722 ± 0.00156	0.375169 ± 0.045204	0.276212 ± 0.043675
UVRA	0.99666 ± 0.00239	0.775236 ± 0.141614	0.715979 ± 0.171639

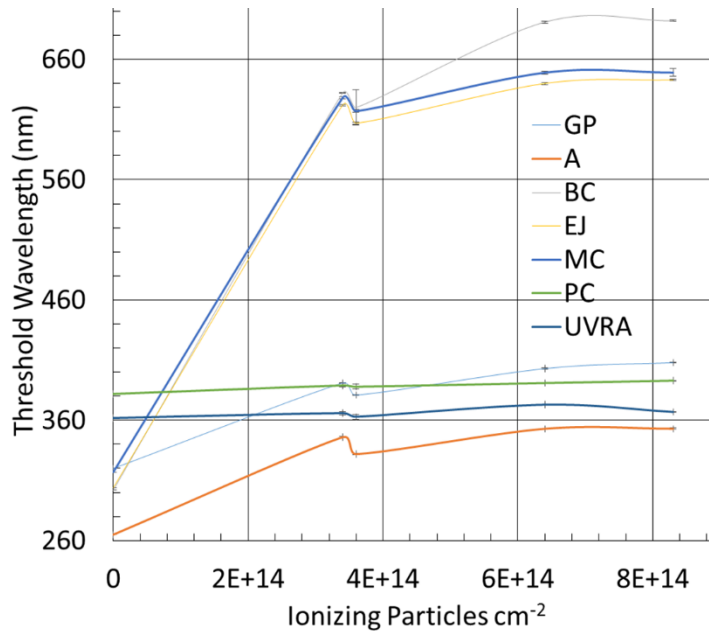


Figure 6: Threshold wavelength as a function of fluence for 20% transmittance.

Results

Figure 6 shows that after heavy radiation exposure, GP and light guide materials are able to maintain 20% transmittance at the shorter wavelengths where PMT's are most sensitive. All materials tested show suppression of short wavelengths in their irradiated transmittance spectrum but this is particularly true for the epoxies we tested. Our experiment has identified a general purpose epoxy with similar properties to traditionally used optical cements that suffers less damage under irradiation.

Benefit

The darkening effect that irradiation has on optical cements requires that detectors in the Booster must be replaced annually. This replacement time is costly to Fermilab as it pulls researchers away from other experiments and prevents detectors from providing valuable data. Having found that GP suffers less damage under irradiation allows for an increase in the duration that a detector can measure losses without the need for removal. Scintillation detectors have traditionally used EJ-500 and BC-600 as optical cements, which each cost on average about \$600 per liter. The cost of GP per liter is approximately \$35, making it almost a factor of 20 less expensive. Pending confirmation of compatibility, the radiation tolerance and cost reduction provides Fermilab and the Department of Energy with an opportunity to save both time and money by using GP as a replacement optical cement.

References

- [1] Eljen Technology, 1300 West Broadway, Sweetwater, TX 79556.
- [2] Sauli, Fabio. "Instrumentation in High Energy Physics," World Scientific, River Edge, NJ 07661, 192.
- [3] McMaster-Carr, 600 N. County Line Rd., Elmhurst, IL 60126-2034.
- [4] Saint-Gobain Crystals, 17900 Greatlakes Pkwy., Hiram, OH 44234.
- [5] System Three Resins, Inc., 3500 W. Valley Hwy. N., Suite 105, Auburn, WA 98001.
- [6] Agilent 8453 UV-visible Spectroscopy System, 5301 Stevens Creek Blvd., Santa Clara, CA 95051.
- [7] Barberis, E. et al. *Nucl. Instrum. and Meth.* A326 (1993) 373- 380.